UNIVERSITY OF AMSTERDAM

UvA-DARE (Digital Academic Repository)

Asymptotic-bound-state model for Feshbach resonances

Tiecke, T.G.; Goosen, M.R.; Walraven, J.T.M.; Kokkelmans, S.J.J.M.F.

DOI
10.1103/PhysRevA.82.042712
Publication date
2010
Document Version
Final published version
Published in
Physical Review A

Link to publication

Citation for published version (APA):
Tiecke, T. G., Goosen, M. R., Walraven, J. T. M., & Kokkelmans, S. J. J. M. F. (2010). Asymptotic-bound-state model for Feshbach resonances. *Physical Review A*, *82*(4), 042712. https://doi.org/10.1103/PhysRevA.82.042712

General rights
It is not permitted to download or to forward/distribute the text or part of it without the consent of the author(s) and/or copyright holder(s), other than for strictly personal, individual use, unless the work is under an open content license (like Creative Commons).

Disclaimer/Complaints regulations
If you believe that digital publication of certain material infringes any of your rights or (privacy) interests, please let the Library know, stating your reasons. In case of a legitimate complaint, the Library will make the material inaccessible and/or remove it from the website. Please Ask the Library: https://uba.uva.nl/en/contact, or a letter to: Library of the University of Amsterdam, Secretariat, P.O. Box 19185, 1000 GD Amsterdam, The Netherlands. You will be contacted as soon as possible.

UvA-DARE is a service provided by the library of the University of Amsterdam (https://dare.uva.nl)

Download date:13 Oct 2026

Asymptotic-bound-state model for Feshbach resonances

T. G. Tiecke,[1,*] M. R. Goosen,[2] J. T. M. Walraven,[1] and S. J. J. M. F. Kokkelmans[2]
[1]*Van der Waals–Zeeman Institute of the University of Amsterdam, 1018 XE The Netherlands*
[2]*Eindhoven University of Technology, P.O. Box 513, 5600 MB Eindhoven, The Netherlands*
(Received 7 July 2010; published 22 October 2010)

We present an asymptotic-bound-state model which can be used to accurately describe all Feshbach resonance positions and widths in a two-body system. With this model we determine the coupled bound states of a particular two-body system. The model is based on analytic properties of the two-body Hamiltonian and on asymptotic properties of uncoupled bound states in the interaction potentials. In its most simple version, the only necessary parameters are the least bound state energies and actual potentials are not used. The complexity of the model can be stepwise increased by introducing threshold effects, multiple vibrational levels, and additional potential parameters. The model is extensively tested on the ^{6}Li-^{40}K system and additional calculations on the ^{40}K-^{87}Rb system are presented.

DOI: 10.1103/PhysRevA.82.042712 PACS number(s): 34.50.−s, 34.20.Cf, 67.85.−d

I. INTRODUCTION

The field of ultracold atomic gases has been rapidly growing during the past decades. One of the main sources of growth is the large degree of tunability allowing employment of ultracold gases as model quantum systems [1,2]. In particular, the strength of the two-body interaction parameter, captured by the scattering length a, can be tuned over many orders of magnitude. A quantum system can be made repulsive ($a > 0$), attractive ($a < 0$), noninteracting ($a = 0$), or strongly interacting ($|a| \to \infty$) in a continuous manner by means of Feshbach resonances [3]. These resonances are induced by external fields: magnetically induced Feshbach resonances are conveniently used for alkali-metal atoms, while optically induced Feshbach resonances seem more promising for, e.g., alkaline-earth-metal atoms. In this paper we consider magnetically induced resonances only.

Feshbach resonances depend crucially on the existence of an internal atomic structure, which can be modified by external fields. For alkali-metal atoms, this structure is initiated by the hyperfine interaction, which can be energetically modified by a magnetic field via the Zeeman interaction. For a given initial spin state, its collision threshold and its two-body bound states depend in general differently on the magnetic field. A Feshbach resonance occurs when the threshold becomes degenerate with a bound state. Accurate knowledge of the Feshbach resonance structure is crucial for experiments.

The two-body system has to be solved to obtain the bound state solutions. Since the interactions have both orbital and spin degrees of freedom, this results in a set of radially coupled Schrödinger equations in the spin basis. The set of equations is referred to as coupled-channel equations [4] and can be solved numerically. Quite often it is far from trivial to obtain reliable predictions for the two-body problem, for several reasons: the *ab initio* interaction potentials are usually not accurate enough to describe ultracold collisions. Therefore these potentials have to be modeled by adding and modifying potential parameters. A full calculation for all spin combinations and all potential variations is very time consuming. Moreover, one can easily overlook some features of the bound state spectrum due to numerical issues such as grid sizes and numerical accuracy. This is also due to a lack of insight into the general resonance structure, which is often not obvious from the numerical results.

Given the above, there is certainly a need for fast and simple models to predict and describe Feshbach resonances, which allow for a detailed insight into the resonance structure. In the last decade various simple models have been developed for ultracold collisions [5–7], which vary significantly in terms of complexity, accuracy, and applicability. In all these models the radial equation plays a central role in describing the Feshbach resonances.

In this paper we present in detail the asymptotic-bound-state model (ABM). This model, briefly introduced in Ref. [8], and extended in Ref. [9], was successfully applied to the Fermi-Fermi mixture of ^{6}Li and ^{40}K. In Ref. [8] the observed loss features were assigned to 13 Feshbach resonances with high accuracy, and the obtained parameters served as an input to a full coupled-channel analysis. The ABM builds on an earlier model by Moerdijk *et al.* [10] for homonuclear systems, which was also applied by Stan *et al.* [11] for heteronuclear systems. This earlier model neglects the mixing of singlet and triplet states, therefore allowing the use of uncoupled orbital and spin states. In the ABM we make use of the radial singlet and triplet eigenstates and include the coupling between them, which is a crucial improvement. When these eigenstates form a complete set, including all bound and virtual states of the potentials for all partial waves, this makes the whole approach in principle exact. In practice, only a limited number of states (parameters) have to be taken into account, to achieve already a high degree of accuracy. On this level it would be very interesting to compare the ABM to other simple models, such as the multichannel quantum defect theory approach in Ref. [7], which also starts from an in-principle exact approach.

We show how we can systematically extend the most simple version of the ABM to predict the width of the Feshbach resonances by including threshold behavior. Additionally, we allow for the inclusion of multiple vibrational levels and parameters for the spatial wave function overlap. The fact that the ABM is computationally light provides the possibility

*Present address: Department of Physics, Harvard University, Cambridge, MA 02138, USA

 ©2010 The American Physical Society

to map out the available Feshbach resonance positions and widths for a certain system, as has been shown in Ref. [9]. Throughout the paper we will use the ^{6}Li-^{40}K mixture as a model system to illustrate all introduced aspects. Additionally, we present ABM calculations on the ^{40}K-^{87}Rb mixture to demonstrate its validity on a more complex system, comparing it with accurate coupled-channel calculations [12]. The case of metastable helium atoms where each atom has an electron spin of $s = 1$ and the interaction occurs through singlet, triplet, and quintet interaction potentials we discuss elsewhere [13].

In the following we describe the ABM (Sec. II) and various methods to obtain the required input parameters. In Sec. III the ABM is applied to the three physical systems and in Sec. IV we introduce the coupling to the open channel to predict the width of Feshbach resonances. In Sec. V we summarize our findings and comment on further extensions of the model.

II. ASYMPTOTIC-BOUND-STATE MODEL

In this section we give a detailed description of the asymptotic-bound-state model. In Sec. II A we start with a general overview of the model, which is described in more detail in Secs. II B–II F.

A. Overview

In the ABM we consider two atoms, α and β, in their electronic ground state. To search for Feshbach resonances we use the effective Hamiltonian [14]

$$\mathcal{H} = \mathcal{H}^{\mathrm{rel}} + \mathcal{H}^{\mathrm{int}}. \tag{1}$$

Here $\mathcal{H}^{\mathrm{rel}} = \mathbf{p}^2/2\mu + \mathcal{V}$ describes the relative motion of the atoms in the center-of-mass frame: the first term is the relative kinetic energy, with μ the reduced mass, the second term the effective interaction potential $\mathcal{V}$. The Hamiltonian $\mathcal{H}^{\mathrm{int}}$ stands for the internal energy of the two atoms.

We will represent $\mathcal{H}^{\mathrm{int}}$ by the hyperfine and Zeeman contributions to the internal energy (Sec. II B). Therefore, $\mathcal{H}^{\mathrm{int}}$ is diagonal in the Breit-Rabi pair basis $\{|\alpha\beta\rangle\}$ with eigen-energies $E_{\alpha\beta}$ and typically dependent on the magnetic field B. The internal states $|\alpha\beta\rangle$ in combination with the quantum number l for the angular momentum of the relative motion define the *scattering channels* $(\alpha\beta,l)$.

Because the effective potential $\mathcal{V}$ is in general not diagonal in the pair basis $\{|\alpha\beta\rangle\}$, the internal states of the atoms can change in collisions. To include the coupling of the channels by $\mathcal{V}$, we transform from the pair basis to a spin basis $\{|\sigma\rangle\}$ in which $\mathcal{H}^{\mathrm{rel}}$ is diagonal. We will restrict ourselves (Sec. II C) to effective potentials $\mathcal{V}$ which are diagonal in S, the quantum number of the total electron spin $\mathbf{S} = \mathbf{s}_\alpha + \mathbf{s}_\beta$, where $\mathbf{s}_\alpha$ and $\mathbf{s}_\beta$ are the electron spins of the colliding atoms. The effective potential can thus be written as $\mathcal{V}(r) = \sum_S |S\rangle V_S(r)\langle S|$, where r is the interatomic separation. The examples discussed in this paper are alkali-metal atoms ($s = 1/2$), which lead to a decomposition into singlet ($S = 0$) and triplet ($S = 1$) potentials.

The eigenstates of $\mathcal{H}^{\mathrm{rel}}$ (bound states and scattering states) are solutions of the Schrödinger equations for a given value of l, using effective potentials $V_S^l(r)$ in which the centrifugal forces are included (Sec. II C). Since the effective potentials are central interactions, a separation of variables can be performed to describe the wave function as a product of a radial and angular part, $|\Psi\rangle = |\psi\rangle|Y_{m_l}^l\rangle$. The ABM solves the Schrödinger equation for the Hamiltonian (1) starting from a restricted set of (typically just a few) *discrete* eigenstates $|\psi_\nu^{Sl}\rangle|Y_{m_l}^l\rangle$ of $\mathcal{H}^{\mathrm{rel}}$, using their binding energies ϵ_ν^{Sl} as free parameters. The continuum states are not used in the model. The set $\{|\psi_\nu^{Sl}\rangle\}$ corresponds to the bound state wave functions $\psi_\nu^{Sl}(r) = \langle r|\psi_\nu^{Sl}\rangle$ in the effective potentials $V_S^l(r)$, with ν and l being the vibrational and rotational quantum numbers, respectively.

The ABM solutions are obtained by diagonalization of the Hamiltonian (1) using the restricted set of bound states $\{|\psi_\nu^{Sl}\rangle|\sigma\rangle\}$. This is equivalent to solving the secular equation

$$\det\left|\left(\epsilon_\nu^{Sl} - E_b\right)\delta_{\nu l\sigma,\nu' l'\sigma'} + \left\langle\psi_\nu^{Sl}\middle|\psi_{\nu'}^{S'l}\right\rangle\langle\sigma|\mathcal{H}^{\mathrm{int}}|\sigma'\rangle\right| = 0, \tag{2}$$

where we have used the orthonormality of $|Y_{m_l}^l\rangle$. The roots E_b represent the eigenvalues of $\mathcal{H}$, which are shifted with respect to the *bare* levels ϵ_ν^{Sl} due to the presence of the coupling term $\mathcal{H}^{\mathrm{int}}$. The roots E_b will be accurate as long as the influence of the continuum solutions is small. Since the bound state wave functions $\psi_\nu^{Sl}(r)$ are orthonormal for a given value of S and l, the Franck-Condon factors are $\langle\psi_\nu^{Sl}|\psi_{\nu'}^{Sl}\rangle = \delta_{\nu\nu'}$. The eigenstates of $\mathcal{H}$ define bound states in the system of *coupled channels*.

We define the *entrance channel* $(\alpha\beta,l)_0$ by the internal states $|\alpha\beta\rangle$ for which we want to find Feshbach resonances with a given angular momentum state of $l = 0,1,\ldots$. The energy $E_{\alpha\beta}^0(B)$ of two free atoms at rest in the entrance channel defines the *threshold energy*, which separates the continuum of scattering states from the discrete set of bound states. In the ABM we define $\mathcal{H}$ relative to this energy. With this convention the threshold energy always corresponds to $E = 0$, irrespective of the magnetic field. Further, we consider only entrance channels that are stable against spin exchange relaxation.

Since in the ABM we consider only bound states, and therefore are in the regime $E < 0$, all channels are energetically *closed*. Collisions in the entrance channel would have a collision energy of $E > 0$ and the entrance channel would be energetically *open*, i.e., the atoms are not bound and have a finite probability of reaching $r = \infty$ in this channel. Although all channels are closed in the ABM we will refer to the entrance channel as the open channel, anticipating the inclusion of threshold effects in Sec. IV.

In Secs. II B–II F we discuss the ABM in its simplest form, where level broadening by coupling to the continuum is neglected [8]. In this approximation, Feshbach resonances are predicted for magnetic fields B_0 where a bound level crosses the threshold, $E_b = \mu_{\mathrm{rel}}(B - B_0)$ with $\mu_{\mathrm{rel}} \equiv \partial E_b/\partial B|_{B=B_0}$, and where coupling to the continuum is in principle allowed by conservation of the angular momentum. To determine the crossings the diagonalization (2) has to be carried out as a function of magnetic field.

The procedure becomes particularly simple when the coupling strength $\mathcal{H}^{\mathrm{int}}$ is small compared to the separation of the rovibrational levels in the various potentials $V_S^l(r)$ because in this case the basis set can be restricted to only the least bound level in each of the potentials $V_S^l(r)$. In this case the set of levels $\{\epsilon_\nu^{Sl}\}$ reduces to a small number

$\{\epsilon^{Sl}\}$, with $|s_\alpha - s_\beta| \leqslant S \leqslant s_\alpha + s_\beta$. In the case of the alkali metals, only two levels ϵ^{0l} and ϵ^{1l} are relevant for each value of l. Further, as will be shown in Sec. II F, the least bound states have the long-range behavior of *asymptotically bound states*, which makes it possible to estimate the value of Franck-Condon factors $\langle\psi_\nu^{Sl}|\psi_{\nu'}^{S'l}\rangle$ without detailed knowledge of the short-range behavior of the potentials $V_S^l(r)$. This reduces the diagonalization (2) to the diagonalization of a spin Hamiltonian. Treating the $\{\epsilon^{Sl}\}$ as fitting parameters, their values can be determined by comparison with a handful of experimentally observed resonances. Once these $\{\epsilon^{Sl}\}$ are known, the position of all Feshbach resonances associated with these levels can be predicted. As this procedure does not involve numerical solution of the Schrödinger equation for the relative motion it provides an enormous simplification over coupled-channel calculations.

In Sec. IV we turn to the extended version of the ABM in which also the coupling to the open channel is taken into account. The presence of such a coupling gives rise to a shift Δ of the uncoupled levels and above threshold to a broadening Γ [9]. The width of a Feshbach resonance is related to the lifetime $\tau = \hbar/\Gamma$ of the bound state above threshold and provides a measure for the coupling to the continuum. In magnetic field units the width ΔB is related to the scattering length by the expression [10]

$$a(B) = a_{\rm bg}\left(1 - \frac{\Delta B}{B - B_0}\right), \tag{3}$$

where $a_{\rm bg}$ is the background scattering length. Interestingly, the width ΔB can also be determined with the same restricted basis set $\{|\psi_\nu^{Sl}\rangle\}$, which does not include continuum states. In Sec. IV this is shown for the simplest case where only a single level is resonant and the resonance width can be found from the coupling of two bound state levels: the resonant level and the least bound level in the entrance channel.

B. Internal energy

To describe the internal energy of the colliding atoms we restrict the atomic Hamiltonian to the hyperfine and Zeeman interactions

$$\mathcal{H}^{\rm A} = \mathcal{H}^{\rm hf} + \mathcal{H}^{\rm Z} \tag{4}$$

$$= \frac{a_{\rm hf}}{\hbar^2}\mathbf{i}\cdot\mathbf{s} + (\gamma_e\mathbf{s} - \gamma_i\mathbf{i})\cdot\mathbf{B}, \tag{5}$$

where $\mathbf{s}$ and $\mathbf{i}$ are the electron and nuclear spins, respectively, γ_e and γ_i are their respective gyromagnetic ratios, $a_{\rm hf}$ is the hyperfine energy, and $\mathbf{B}$ is the externally applied magnetic field. The hyperfine interaction couples the electron and nuclear spins, which add to a total angular momentum $\mathbf{f} = \mathbf{s} + \mathbf{i}$. In Fig. 1 the well-known Breit-Rabi diagrams of ^{6}Li and ^{40}K are shown, the curves corresponding to the eigenvalues of $\mathcal{H}^{\rm A}$. The one-atom hyperfine states are labeled $|fm_f\rangle$, although f is a good quantum number only in the absence of an external magnetic field.

By labeling the colliding atoms with α and β, the two-body internal Hamiltonian becomes $\mathcal{H}^{\rm int} = \mathcal{H}_\alpha^{\rm A} + \mathcal{H}_\beta^{\rm A}$, and the spin state of the colliding pair can be described in the Breit-Rabi pair basis $|\alpha\beta\rangle \equiv |f_\alpha m_{f_\alpha}, f_\beta m_{f_\beta}\rangle \equiv |f,m_f\rangle_\alpha \otimes |f,m_f\rangle_\beta$. The

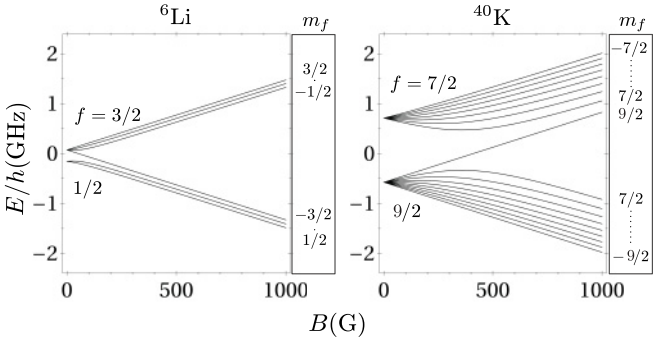

FIG. 1. Single-atom hyperfine diagrams for ^{6}Li and ^{40}K. The curves correspond to the eigenvalues of $\mathcal{H}^{\rm A}$ and are labeled by the zero-field quantum numbers $|fm_f\rangle$.

corresponding energy of two free atoms at rest defines the B-dependent threshold energy introduced in Sec. II A.

C. Relative Hamiltonian

The bound eigenstates of $\mathcal{H}^{\rm rel}$ play a central role in the determination of the coupled bound states $\mathcal{H}$ responsible for the Feshbach resonances. The relative Hamiltonian includes the effective interaction $\mathcal{V}$ resulting from all Coulomb interactions between the nuclei and electrons of both atoms.[1] This effective interaction is isotropic and depends only on the quantum number S associated with the total electron spin. For these central potentials the two-body solutions will depend on the orbital quantum number l, but not on its projection m_l. In the absence of any anisotropic interaction both l and m_l are good quantum numbers of $\mathcal{H}^{\rm rel}$ and $\mathcal{H}$.

We specify the ABM basis states as $\{|\psi_\nu^{Sl}\rangle|\sigma\rangle\}$. Here the spin basis states $|\sigma\rangle \equiv |SM_S\mu_\alpha\mu_\beta\rangle$ are determined by the spin quantum number S and the magnetic quantum numbers M_S, μ_α, and μ_β of the $\mathbf{S}$, $\mathbf{i}_\alpha$, and $\mathbf{i}_\beta$ operators, respectively. The sum $M_F = M_S + \mu_\alpha + \mu_\beta$ is conserved by the Hamiltonian $\mathcal{H}$. This limits the number of spin states which have to be included in the set $|\sigma\rangle$. The bound state wave functions $\psi_\nu^{Sl}(r)$ for the singlet and triplet potentials, characterized by the vibrational and rotational quantum numbers ν and l, satisfy the reduced radial wave equation of $\mathcal{H}^{\rm rel}$ for specific values of S and l,

$$\left(-\frac{\hbar^2}{2\mu}\frac{d^2}{dr^2} + V_S^l(r)\right)\psi_\nu^{Sl}(r) = \epsilon_\nu^{Sl}\psi_\nu^{Sl}(r). \tag{6}$$

Here $V_S^l(r) \equiv V_S(r) + l(l+1)\hbar^2/(2\mu r^2)$ represents the interaction potentials including the centripetal forces. The corresponding binding energies are given by ϵ_ν^{Sl}. In this paper we mainly focus on heteronuclear systems; however, the ABM works equally well for homonuclear systems. In the latter case one would rather use a symmetrized spin basis $|\sigma\rangle \equiv |SM_S I M_I\rangle$, where I is the total nuclear spin and M_I is the magnetic quantum number for $\mathbf{I} = \mathbf{i}_\alpha + \mathbf{i}_\beta$ as described in Ref. [10].

[1]The much weaker magnetic dipole-dipole interactions are neglected.

D. Diagonalization of $\mathcal{H}$

In the ABM basis $\{|\psi_\nu^{Sl}\rangle|\sigma\rangle\}$ the Zeeman term $\mathcal{H}_Z$ is diagonal, with

$$E_\sigma^Z = \langle\sigma|\mathcal{H}_Z|\sigma\rangle = \hbar(\gamma_e M_S - \gamma_\alpha\mu_\alpha - \gamma_\beta\mu_\beta)B \qquad (7)$$

the Zeeman energy of state $|\sigma\rangle$. As the orbital angular momentum is conserved, we can solve Eq. (2) separately for every l subspace. Since the set $\{|\psi_\nu^{Sl}\rangle|\sigma\rangle\}$ is orthonormal the secular equation takes (for a given value of l) the form

$$\det\left|\left(\epsilon_\nu^{Sl} + E_\sigma^Z - E_b\right)\delta_{\nu\sigma,\nu'\sigma'} + \eta_{\nu,\nu'}^{S,S'}\langle\sigma|\mathcal{H}_{\rm hf}|\sigma'\rangle\right| = 0, \quad (8)$$

where $\eta_{\nu,\nu'}^{S,S'} = \langle\psi_\nu^{Sl}|\psi_{\nu'}^{S'l}\rangle$ are Franck-Condon factors between the different S states, which are numbers in the range $0 \leqslant |\eta_{\nu,\nu'}^{S,S'}| \leqslant 1$ for $S \neq S'$ and $\eta_{\nu,\nu'}^{S,S} = \delta_{\nu,\nu'}$. Repeating the procedure as a function of magnetic field, the energy level diagram of all bound states in the system of coupled channels is obtained.

It is instructive to separate the hyperfine contribution into two parts, $\mathcal{H}_{\rm hf} = \mathcal{H}_{\rm hf}^+ + \mathcal{H}_{\rm hf}^-$, where

$$\mathcal{H}_{\rm hf}^\pm = \frac{a_{\rm hf}^\alpha}{2\hbar^2}(\mathbf{s}_\alpha \pm \mathbf{s}_\beta)\cdot\mathbf{i}_\alpha \pm \frac{a_{\rm hf}^\beta}{2\hbar^2}(\mathbf{s}_\alpha \pm \mathbf{s}_\beta)\cdot\mathbf{i}_\beta. \qquad (9)$$

Because $\mathcal{H}_{\rm hf}^+$ conserves S, it couples the ABM states only within the singlet and triplet manifolds. The term $\mathcal{H}_{\rm hf}^-$ is off diagonal in the ABM basis, and hence couples singlet to triplet. Accordingly, also the hyperfine term in the secular equation separates into two parts,

$$\eta_{\nu,\nu'}^{S,S'}\langle\sigma|\mathcal{H}_{\rm hf}|\sigma'\rangle = \delta_{\nu,\nu'}\langle\sigma|\mathcal{H}_{\rm hf}^+|\sigma'\rangle + \eta_{\nu,\nu'}^{S,S'}\langle\sigma|\mathcal{H}_{\rm hf}^-|\sigma'\rangle. \qquad (10)$$

Note that the second term of Eq. (10) is zero *unless* $S \neq S'$. This term was neglected in the models of Refs. [10,11]. This is a good approximation if no Feshbach resonances occur near magnetic fields, where the energy difference between singlet and triplet levels is on the order of the hyperfine energy. However, for a generic case this term cannot be neglected.

To demonstrate the procedure of identification of Feshbach resonances, we show in Fig. 2 the ABM solutions for a simple fictitious homonuclear system with $S = 1$ and $I = 2$ for an entrance channel with $M_F = M_S + M_I = 0$ and $l = 0$. The example has the spin structure of ^{6}Li but we use ABM parameters ϵ^0, ϵ^1, and η^{01}, with values chosen for convenience of illustration. The field dependence of threshold energy of the entrance channel $E_{\alpha\beta}^0$ is shown here explicitly (dashed line). The energies E_b (solid lines) are labeled by their high-field quantum numbers $|SM_SIM_I\rangle$, and the binding energies in the singlet and triplet potentials are chosen to be $\epsilon^0 = -10$ and $\epsilon^1 = -5$. The avoided crossings around $B = 0$ are caused by the hyperfine interaction and are proportional to $a_{\rm hf}$; the avoided crossing between the singlet and triplet levels is proportional to the wave function overlap η^{01}. Four s-wave Feshbach resonances occur, indicated at the crossings 1, 2, and 3 (double resonance). The resonances at 1 and 2 are mostly determined by the triplet binding energy ϵ^1 and the resonances at 3 by the singlet binding energy ϵ^0.

E. Free parameters

The free parameters of the ABM are the binding energies $\epsilon_\nu^{S,l}$ and the Franck-Condon factors $\eta_{\nu,\nu'}^{S,S'}$. These parameters

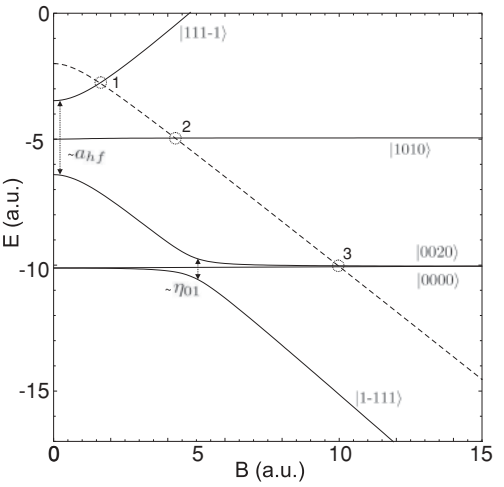

FIG. 2. ABM calculation for a fictitious homonuclear system with $S = 1$ and $I = 2$ for an entrance channel with $M_F = M_S + M_I = 0$ and $l = 0$. The threshold energy of the entrance channel $E_{\alpha\beta}^0$ is shown here explicitly as the dashed line. The energies E_b (solid lines) are labeled by their high-field quantum numbers $|SM_SIM_I\rangle$. The binding energies of the least bound states in the singlet and triplet potentials are chosen to be $\epsilon^0 = -10$ and $\epsilon^1 = -5$. The avoided crossing around $B = 0$ is proportional to the hyperfine interaction $a_{\rm hf}$ and those between the singlet and triplet levels to the wave function overlap η_{01} and the hyperfine interaction $a_{\rm hf}$. Four Feshbach resonances occur indicated at the crossings 1, 2, and 3 (double resonance).

can be obtained in a variety of manners. Here we discuss three methods, two of which will be demonstrated in Sec. III and the third in Ref. [13].

First, if the scattering potentials $V_S^l(r)$ are very well known, the bound state wave functions of the vibrational levels can be obtained by solving Eq. (6) for $\epsilon_\nu^{Sl} < 0$. Numerical values of the Franck-Condon factors follow from the obtained eigenfunctions. This method is very accurate and can be extended to deeply bound levels; however, accurate model potentials are available for only a limited number of systems.

A second method can be used when the potentials are not very well or only partially known. For large interatomic distances the potentials can be parametrized by the dispersion potential

$$V(r) = -\frac{C_6}{r^6}. \qquad (11)$$

Since this expression is not correct for short distances, we account for the inaccurate inner part of the potential by a boundary condition based on the accumulated phase method [15]. This boundary condition has a one-to-one relationship to the interspecies s-wave singlet and triplet scattering lengths. This approach requires only three input parameters: the van der Waals C_6 coefficient and the singlet (a_S) and triplet (a_T) scattering lengths. For an accurate description involving deeper bound states, the accumulated phase boundary condition can be made more accurate by including additional parameters [15].

The third method to obtain the free parameters is by direct comparison of ABM predictions with experimentally observed Feshbach resonances, for instance obtained in a search for loss features in an ultracold atomic gas. A loss feature spectrum

can be obtained by measuring, as a function of magnetic field, the remaining number of atoms after a certain holding time at fixed magnetic field. The ABM parameters follow by a fitting procedure yielding the best match of the predicted threshold crossing fields with the observed loss feature spectrum. We applied this method in Ref. [8], where it has proven to be very powerful for rapid assignment of Feshbach resonances in the ^{6}Li-^{40}K mixture due to the small computational time required to diagonalize a spin Hamiltonian.

The number of fit parameters is determined by the number of bound states that have to be considered. Depending on the atomic species and the magnetic field, only a selected number of vibrational levels ϵ_v^{Sl} have to be taken into account. This number can be estimated by considering the maximum energy range involved. An upper bound results from comparing the maximum dissociation energy of the least bound vibrational level D^* with the maximum internal energy of the atom pair $E_{\mathrm{int,max}}$. The maximum dissociation energy of the vth vibrational level can be estimated semiclassically [16] as

$$D^* = \left(\frac{v\zeta\hbar}{\mu^{1/2}C_6^{1/6}}\right)^3, \tag{12}$$

where $\zeta = 2[\Gamma(1+1/6)/\Gamma(1/2+1/6)] \simeq 3.434$, v being counted from the dissociation limit, i.e., $v=1$ is the least bound state. The maximum internal energy is given by the sum of the hyperfine splitting of each of the two atoms at zero field, the maximum Zeeman energy for the free atom pair and the maximum Zeeman energy for the molecule:

$$E_{\mathrm{int,max}} \simeq E_{\mathrm{hf}}^{\alpha} + E_{\mathrm{hf}}^{\beta} + 2(s_\alpha + s_\beta)g_S\mu_B B, \tag{13}$$

where $E_{\mathrm{hf}}^{\alpha,\beta} = a_{\mathrm{hf}}^{\alpha,\beta}(i_{\alpha,\beta} + s_{\alpha,\beta})$ and we have neglected the nuclear Zeeman effect. Comparing Eqs. (12) and (13) gives us an expression for the number of vibrational levels N_v which have to be considered,

$$N_v \simeq \left\lceil \frac{\mu^{1/2}C_6^{1/6}}{\hbar\zeta} E_{\mathrm{int,max}}^{1/3} \right\rceil, \tag{14}$$

where $\lceil x \rceil$ denotes the smallest integer not less than the argument x. The maximum possible magnetic field B_{max} required to encounter a Feshbach resonance can be estimated from Eq. (12) by neglecting the hyperfine energy as

$$B_{\mathrm{max}} \simeq \frac{D^*}{(s_\alpha + s_\beta)g_S\mu_B}; \tag{15}$$

here we assumed an (unfavorable) spin mixture where either the threshold or the bound level does not shift with respect to the magnetic field. If the hyperfine energy is comparable to or larger than the vibrational level splitting D^*, the expression for B_{max} overestimates the maximum field of the lowest-field Feshbach resonance.

F. Asymptotic bound states

The most crucial ABM parameters are the binding energies ϵ_v^{Sl}. However, for accurate predictions of the Feshbach resonance positions the Franck-Condon factors also have to be accurate. For weakly bound states, these factors are mainly determined by the difference in binding energy of the overlapping states, rather than by the potential shape. Therefore good approximations can be made with little knowledge of the scattering potential.

For very weakly bound states, the outer classical turning point r_c is found at distances $r_c \gg r_0$; i.e., far beyond the van der Waals radius of the interaction potential,

$$r_0 = \frac{1}{2}\left(\frac{2\mu C_6}{\hbar^2}\right)^{1/4}. \tag{16}$$

These states are called *halo states* [17]. Because in this case most of the probability density of the wave function is found outside the outer classical turning point, these states can be described by a zero-range potential with a wave function of the type $\psi(r) \sim e^{-\kappa r}$, where $\kappa = (-2\mu\epsilon/\hbar^2)^{1/2}$ is the wave number corresponding to a bound state with binding energy ϵ. The Franck-Condon factor of two halo states with wave numbers κ_0 and κ_1 is given by

$$\langle\psi^0|\psi^1\rangle = 2\frac{\sqrt{\kappa_0\kappa_1}}{\kappa_0+\kappa_1}. \tag{17}$$

This approximation is valid for binding energies $|\epsilon| \ll C_6/r_0^6$.

The calculation of the Franck-Condon factors can be extended to deeper bound states by including the dispersive van der Waals tail. For distances $r \gg r_X$, where r_X is the exchange radius, the potential is well described by Eq. (11), and the Franck-Condon factors can be calculated by numerically solving the Schrödinger equation (6) for the van der Waals potential (11) on the interval $r_X < r < \infty$ [18]. The exchange radius r_X is defined as the distance where the van der Waals interaction equals the exchange interaction. This method can be used for *asymptotic bound states*, which we define by the condition $r_c > r_X$. If even deeper bound states, with $r_c < r_X$, have to be taken into account, the potential can be extended by including the exchange interaction [19] or by using full model potentials.

To illustrate the high degree of accuracy achieved by using asymptotic bound states, we calculate the Franck-Condon factor for a contact potential (halo states), a van der Waals potential (asymptotic bound states), and a full model potential including short-range behavior, derived from Refs. [20,21]. Figure 3 shows the Franck-Condon factor η_{11}^{01} for ^{6}Li-^{40}K calculated numerically for the model potential and the van der Waals potential, and analytically using Eq. (17). The van der Waals coefficient used is $C_6 = 2322E_ha_0^6$ [22], where $E_h = 4.359\,74 \times 10^{-18}$ J and $a_0 = 0.052\,917\,72$ nm. The value of η_{11}^{01} has been plotted as a function of the triplet binding energy ϵ^1 for three different values of the singlet binding energy ϵ^0. It is clear that the contact potential is applicable only for $\epsilon/h \lesssim 100$ MHz; hence only for systems with resonant scattering in the singlet and triplet channels.

The approximation based on the C_6 potential yields good agreement down to binding energies of $\epsilon/h \lesssim 40$ GHz, which is much more than the maximum possible vibrational level splitting of the least bound states ($D^*/h = 8.2$ GHz), and hence is sufficient to describe Feshbach resonances originating for the least bound vibrational level. The black circle indicates the actual Franck-Condon factor for the least bound state of ^{6}Li-^{40}K. For the contact, van der Waals, and model potentials we find $\eta_{11}^{01} = 0.991$, $\eta_{11}^{01} = 0.981$, and $\eta_{11}^{01} = 0.979$, respectively.

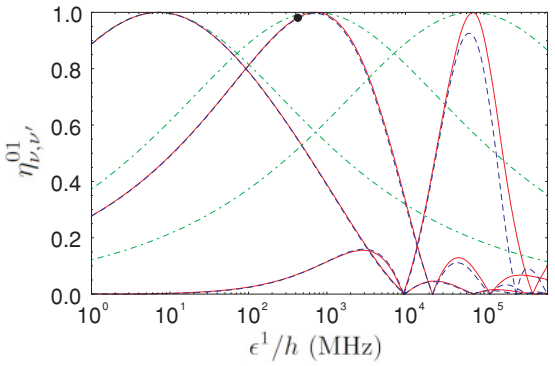

FIG. 3. (Color online) Franck-Condon factor $\eta^{01}_{\nu,\nu'}$ for the least bound states of the ^{6}Li-^{40}K system, calculated as a function of the triplet binding energy ϵ^1 for three different values of $\epsilon^0/h = 7.16$, 716, and 7.16×10^4 MHz. $\eta^{01}_{\nu,\nu'}$ is calculated for the model potential (dashed blue), the $-C_6/r^6$ potential (solid red), and the contact potential, Eq. (17) (dash-dotted green). The black circle indicates the actual value for the least bound state of ^{6}Li-^{40}K ($\epsilon^0/h = 716$ MHz and $\epsilon^1/h = 425$ MHz). The nodes in $\eta^{01}_{\nu,\nu'}$ correspond approximately to the appearance of deeper-lying vibrational states, i.e., for $\epsilon^1/h \gtrsim 10^4$ MHz, $\nu > 1$.

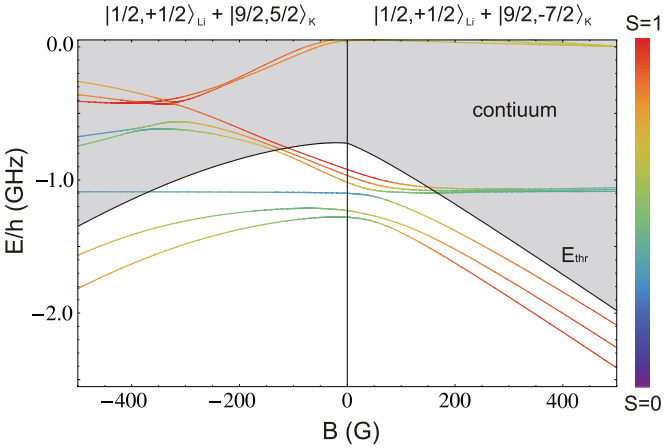

FIG. 4. (Color online) Energies of all the coupled bound states for ^{6}Li-^{40}K with total spin $M_F = \pm 3$. The black solid line indicates the threshold energy of the entrance channel $|1/2, +1/2\rangle_{Li} \otimes |9/2, +5/2\rangle_K$ for $B < 0$ and $|1/2, +1/2\rangle_{Li} \otimes |9/2, -7/2\rangle_K$ for $B > 0$. The gray area represents the scattering continuum and the (colored) lines indicate the coupled bound states. Feshbach resonances occur when a bound state crosses the threshold energy. The color scheme indicates the admixture of singlet and triplet contributions in the bound states obtained from the eigenstates of the Hamiltonian (1). The strong admixture near the threshold crossings at $B \simeq 150$ G demonstrates the importance of the singlet-triplet mixing in describing Feshbach resonance positions accurately. Since in these calculations the coupled bound states are not coupled to the open channel, they exist even for energies above the threshold.

III. APPLICATION TO VARIOUS SYSTEMS

In this section we demonstrate the versatility of the ABM by applying it to two different systems using the different approaches as discussed in Sec. II E.

A. ^{6}Li-^{40}K

Both ^{6}Li and ^{40}K have electron spin $s = 1/2$; therefore the total electron spin can be singlet $S = 0$ or triplet $S = 1$. We intend to describe all loss features observed in Ref. [8]. Since all these features were observed for magnetic fields below 300 G, we find that, by use of Eq. (14), it is sufficient to take into account only the least bound state ($\nu = 1$) of the singlet and triplet potentials. This reduces the number of fit parameters to $\epsilon^{Sl}_\nu = \epsilon^{0,l}_1$ and $\epsilon^{1,l}_1$. Subsequently, we calculate the rotational shifts by parametrizing the $l > 0$ bound state energies with the aid of model potentials[2] as described by [20,21]. This allows us to reduce the number of binding energies to be considered to only two: $\epsilon^{0,0}_1 \equiv \epsilon^0$ and $\epsilon^{1,0}_1 \equiv \epsilon^1$. We now turn to the Franck-Condon factor η^{01}_{11} of the two bound states. As discussed in Sec. II F its value is $\eta^{01}_{11} = 0.979$ and can be taken along in the calculation or approximated as unity. We first consider the case of $\eta^{01}_{11} \equiv 1$; this reduces the total number of fit parameters to only two. We fit the positions of the threshold crossings to the 13 observed loss features reported in Ref. [8] by minimizing the χ^2 value while varying ϵ^0 and ϵ^1. We obtain optimal values of $\epsilon^0/h = 716(15)$ MHz and $\epsilon^1/h = 425(5)$ MHz, where the error bars indicate one standard deviation. In Fig. 4, the threshold and spectrum of coupled bound states with $M_F = +3$ (-3) is shown for positive (negative) magnetic field values. The color scheme indicates the admixture of singlet and triplet contributions in the bound states. Feshbach resonances will occur at magnetic fields where the energy of the coupled bound states and the scattering threshold match. The strong admixture of singlet and triplet contributions at the threshold crossings emphasizes the importance of including the singlet-triplet mixing term $\mathcal{H}^-_{hf}$ in the Hamiltonian. All 13 calculated resonance positions have good agreement with the coupled-channel calculations as described in Ref. [8], verifying that the ABM yields a good description of the threshold behavior of the ^{6}Li-^{40}K system for the studied field values.

We repeat the χ^2 fitting procedure now including the numerical value of the overlap. The values of η^{01}_{11} for both the s-wave and p-wave bound states are calculated numerically while varying ϵ^0 and ϵ^1. This fit results in a slightly larger χ^2 value with corresponding increased discrepancies in the resonance positions. However, all of the calculated resonance positions are within the experimental widths of the loss features. Therefore, the analysis with $\eta^{01}_{11} \equiv 1$ and $\eta^{01}_{11} = 0.979$ can be safely considered to yield the same results within the experimental accuracy.

B. ^{40}K-^{87}Rb

We now turn to the ^{40}K-^{87}Rb mixture to demonstrate the application of the ABM to a system including multiple (three) vibrational levels in each potential and the corresponding nontrivial values for the Franck-Condon factors. We consider s-wave ($l = 0$) resonances. Although accurate K-Rb scattering potentials are known [23], we choose to use the accumulated phase method as discussed in Sec. II E using only three ABM

[2]Note that this procedure can also be applied with only a C_6 coefficient by utilizing the accumulated phase method.

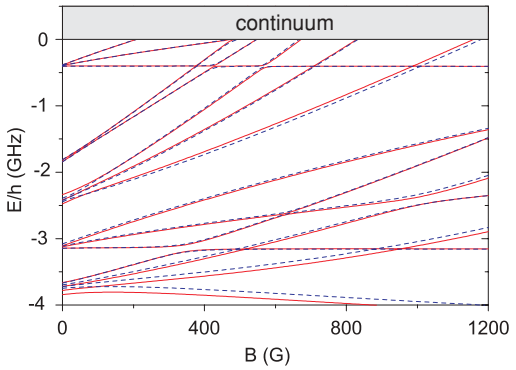

FIG. 5. (Color online) Bound state spectrum for ^{40}K-^{87}Rb for $M_F = -7/2$ plotted with respect to the threshold energy $E^0_{\mathrm{K,Rb}}$ of the $|9/2, -9/2\rangle_{\mathrm{K}} + |1,1\rangle_{\mathrm{Rb}}$ mixture. Solid red lines are ABM calculations and the blue dashed lines are numerical coupled-channel calculations. Good agreement between the two calculations is found, in particular for the weakest bound levels.

parameters to demonstrate the accuracy of the ABM for a more complex system like ^{40}K-^{87}Rb.

We solve the reduced radial wave equation (6) for $V_S(r) = -C_6/r^6$ and the continuum state $E = \hbar^2k^2/2\mu$ in the limit $k \to 0$. We obtain the accumulated phase boundary condition at $r_{\mathrm{in}} = 18a_0$ from the boundary condition at $r \to \infty$ using the asymptotic s-wave scattering phase shift $\delta_0 = \arctan(-ka)$, where a is the known singlet or triplet scattering length. Subsequently, we obtain binding energies for the three last bound states of the singlet and triplet potential by solving the same equation (6) but now using the accumulated phase at $r = r_{\mathrm{in}}$ and $\psi(r \to \infty) = 0$ as boundary conditions. We numerically calculate the Franck-Condon factors by normalizing the wave functions for $r_{\mathrm{in}} < r < r_\infty$, thereby neglecting the wave function in the inner part of the potential ($0 < r < r_{\mathrm{in}}$). This approximation becomes less valid for more deeply bound states. We use as input parameters $C_6 = 4274E_h a_0^6$ [22], $a_S = -111.5a_0$, and $a_T = -215.6a_0$ [23]. Figure 5 shows the spectrum of bound states with respect to the threshold energy for the spin mixture of $|f,m_f\rangle = |9/2, -9/2\rangle_{\mathrm{K}}$ and $|1,1\rangle_{\mathrm{Rb}}$ states. The red curves indicate the ABM results and the blue curves correspond to full coupled-channel calculations [24]. The agreement between the two models is satisfactory, especially for the weakest bound states close to the threshold. A conceptually different analysis of the K-Rb system using also only three input parameters has been performed by Hanna *et al.* [7].

IV. FESHBACH RESONANCE WIDTH

A. Overview

The asymptotic-bound-state model has been used so far to determine the position of the Feshbach resonances but not their width. As is well known from standard Feshbach theory, the width of s-wave resonances depends on the coupling between the resonant level and the continuum [25,26]. For resonances with $l > 0$ the width is determined by a physically different process, namely, tunneling through the centrifugal barrier. Here we discuss only the width of s-wave resonances. We determine the resonance width by analyzing the shift of the resonant level close to threshold due to the coupling with the least bound state of the open channel. This is possible using again the restricted basis set of bound states $\{|\psi_\nu^{Sl}\rangle|\sigma\rangle\}$, introduced in Sec. II. The possibility of obtaining the resonance width by analyzing the shift is plausible because near a resonance the scattering behavior in the zero-energy limit is closely related to the threshold behavior of the bound state. To reveal the coupling as contained in the ABM approximation, we partition the total Hilbert space of the Hamiltonian (1) into two orthogonal subspaces $\mathcal{P}$ and $\mathcal{Q}$. The states of the open channels are located in $\mathcal{P}$ space, those of the closed channels in $\mathcal{Q}$ space [10]. This splits the Hamiltonian $\mathcal{H}$ into four parts (cf. Sec. IV B): $\mathcal{H} = \mathcal{H}_{PP} + \mathcal{H}_{PQ} + \mathcal{H}_{QP} + \mathcal{H}_{QQ}$. Here $\mathcal{H}_{PP}$ and $\mathcal{H}_{QQ}$ describe the system within each subspace and $\mathcal{H}_{PQ}$ ($= \mathcal{H}_{QP}^\dagger$) describe the coupling between the $\mathcal{P}$ and $\mathcal{Q}$ spaces, thus providing a measure for the coupling between the open channels in $\mathcal{P}$ space and the closed channels in $\mathcal{Q}$ space.

The scattering channels are defined by the Breit-Rabi pair states $|\alpha\beta\rangle = |f_\alpha m_{f_\alpha}, f_\beta m_{f_\beta}\rangle$. In the associated pair basis the diagonal matrix elements of the Hamiltonian $\mathcal{H}$ correspond to the "bare" binding energies of the pair states; i.e., the binding energy in the absence of coupling between the channels by $V(r)$. Restricting ourselves, for purposes of introduction, to a single open channel and to the least bound states in the interaction potentials, $\mathcal{H}_{PP}$ is a single matrix element on the diagonal of $\mathcal{H}$, corresponding to the *bare* binding energy of the least bound state of the entrance channel, $\epsilon_P = -\hbar^2\kappa_P^2/2\mu$. The energy ϵ_P can be readily calculated by projecting the pair state on the spin basis $\{|\sigma\rangle = |SM_s\mu_\alpha\mu_\beta\rangle\}$, and is given by

$$\epsilon_P = \sum_S \epsilon_\nu^{Sl} \sum_{M_S,\mu_\alpha,\mu_\beta} \langle SM_s\mu_\alpha\mu_\beta|f_\alpha m_{f_\alpha}, f_\beta m_{f_\beta}\rangle^2. \quad (18)$$

In the following sections we will show that the width ΔB of the resonance is a function of the bare binding energy ϵ_P of the entrance channel and a single matrix element of $\mathcal{H}_{PQ}$, denoted by $\mathcal{K}$, representing the coupling of the level ϵ_P to the resonant level in $\mathcal{Q}$ space. We will show that the width is given by the expression

$$\mu_{\mathrm{rel}}\Delta B = \frac{\mathcal{K}^2}{2a_{bg}\kappa_P|\epsilon_P|}. \quad (19)$$

Hence, once the ABM parameters are known, the width of the resonances follows with an additional unitary transformation of the ABM matrix to obtain the coupling coefficient $\mathcal{K}$. In view of the orthogonality of the subspaces $\mathcal{P}$ and $\mathcal{Q}$, the submatrix $\mathcal{H}_{QQ}$, corresponding to all closed channels, can be diagonalized, leaving $\mathcal{H}_{PP}$ unaffected but changing the $\mathcal{H}_{PQ}$ and $\mathcal{H}_{QP}$ submatrices. In diagonalized form the $\mathcal{H}_{QQ}$ submatrix contains the energies ϵ_Q of all bound levels in $\mathcal{Q}$ space and includes the coupling of all channels except the coupling to $\mathcal{P}$ space. This transformation allows one to identify the resonant bound state and the corresponding off-diagonal matrix element $\mathcal{K}$ in $\mathcal{H}_{PQ}$, which is a measure for the resonance width. Thus we can obtain the coupling between the open and closed channels without the actual use of continuum states.

In Sec. IV B we present the Feshbach theory tailored to suit the ABM. We give a detailed description of the resonant coupling, and demonstrate with a two-channel model how

the ABM bound state energy E_b compares to the associated $\mathcal{P}$-space bare energy ϵ_P, and to the dressed level in the entrance channel from which one can deduce the resonance width. In Sec. IV C we generalize the results such that the width of the Feshbach resonances can be obtained for the general multichannel case. For a more thorough treatment of the Feshbach formalism, we refer the reader to [25,26], and for its application to cold atom scattering, e.g., [10].

B. Tailored Feshbach theory

By introducing the projector operators P and Q, which project onto the subspaces $\mathcal{P}$ and $\mathcal{Q}$, respectively, the two-body Schrödinger equation can be split into a set of coupled equations [10]

$$(E-\mathcal{H}_{PP})|\Psi_P\rangle = \mathcal{H}_{PQ}|\Psi_Q\rangle, \tag{20}$$

$$(E-\mathcal{H}_{QQ})|\Psi_Q\rangle = \mathcal{H}_{QP}|\Psi_P\rangle, \tag{21}$$

where $|\Psi_P\rangle \equiv P|\Psi\rangle$, $|\Psi_Q\rangle \equiv Q|\Psi\rangle$, $\mathcal{H}_{PP} \equiv P\mathcal{H}P$, $\mathcal{H}_{PQ} \equiv P\mathcal{H}Q$, etc. Within $\mathcal{Q}$ space the Hamiltonian $\mathcal{H}_{QQ}$ is diagonal with eigenstates $|\phi_Q\rangle$ corresponding to the two-body bound state with eigenvalues ϵ_Q. The energy $E = \hbar^2k^2/2\mu$ is defined with respect to the open channel dissociation threshold.

We consider one open channel and assume that near a resonance it couples to a single closed channel. This allows us to write the S matrix of the effective problem in $\mathcal{P}$ space as [10]

$$S(k) = S_P(k)\left(1 - 2\pi i \frac{|\langle\phi_Q|\mathcal{H}_{QP}|\Psi_P^+\rangle|^2}{E-\epsilon_Q-\mathcal{A}(E)}\right), \tag{22}$$

where $|\Psi_P^+\rangle$ are scattering eigenstates of $\mathcal{H}_{PP}$, and $S_P(k)$ is the direct scattering matrix describing the scattering process in $\mathcal{P}$ space in the absence of coupling to $\mathcal{Q}$ space.

The complex energy shift $\mathcal{A}(E)$ describes the dressing of the bare bound state $|\phi_Q\rangle$ by the coupling to the $\mathcal{P}$ space and is represented by

$$\mathcal{A}(E) = \left\langle \phi_Q|\mathcal{H}_{QP}\frac{1}{E^+-\mathcal{H}_{PP}}\mathcal{H}_{PQ}|\phi_Q\right\rangle, \tag{23}$$

where $E^+ = E + i\delta$ with δ approaching zero from positive values. Usually the open channel propagator $[E^+ - \mathcal{H}_{PP}]^{-1}$ is expanded to a complete set of eigenstates of $\mathcal{H}_{PP}$, where the dominant contribution comes from scattering states. To circumvent the use of scattering states we expand the propagator to Gamow resonance states, which leads to a Mittag-Leffler expansion [27]

$$\frac{1}{E^+-\mathcal{H}_{PP}} = \frac{\mu}{\hbar^2}\sum_{n=1}^{\infty}\frac{|\Omega_n\rangle\langle\Omega_n^D|}{k_n(k-k_n)}, \tag{24}$$

where n runs over all poles of the S_P matrix. The Gamow state $|\Omega_n\rangle$ is an eigenstate of $\mathcal{H}_{PP}$ with eigenvalue $\epsilon_{P_n} = \hbar^2k_n^2/(2\mu)$. Correspondingly, the dual state $|\Omega_n^D\rangle \equiv |\Omega_n\rangle^*$ is an eigenstate of $\mathcal{H}_{PP}^\dagger$ with eigenvalue $(\epsilon_{P_n})^*$. Using these dual states, the Gamow states form a biorthogonal set such that $\langle\Omega_n^D|\Omega_{n'}\rangle = \delta_{nn'}$. For bound state poles $k_n = i\kappa_n$, where $\kappa_n > 0$, Gamow states correspond to properly normalized bound states.

We assume the scattering in the open channel is dominated by a single bound state ($k_n = i\kappa_P$). This allows us to write the direct scattering matrix in Eq. (22) as

$$S_P(k) = e^{-2ika_{\rm bg}} = e^{-2ika_{\rm bg}^P}\frac{\kappa_P - ik}{\kappa_P + ik}, \tag{25}$$

where $a_{\rm bg}$ is the open channel scattering length, and the P-channel background scattering length $a_{\rm bg}^P$ is on the order of the range of the interaction potential, $a_{\rm bg}^P \approx r_0$. Since we only have to consider one bound state pole (with energy ϵ_P) in $\mathcal{P}$ space, the Mittag-Leffler series Eq. (24) is reduced to only one term. Therefore, the complex energy shift Eq. (23) reduces to

$$\mathcal{A}(E) = \frac{\mu}{\hbar^2}\frac{-iA}{\kappa_P(k-i\kappa_P)}, \tag{26}$$

where $A \equiv \langle\phi_Q|\mathcal{H}_{QP}|\Omega_P\rangle\langle\Omega_P^D|\mathcal{H}_{PQ}|\phi_Q\rangle$ is a positive constant. The coupling matrix element between open channel bound state and closed channel bound state responsible for the Feshbach resonance is related to A.

The complex energy shift can be decomposed into a real and an imaginary part such that $\mathcal{A}(E) = \Delta_{\rm res}(E) - \frac{i}{2}\Gamma(E)$. For energies $E > 0$ the unperturbed bound state becomes a quasibound state: its energy undergoes a shift $\Delta_{\rm res}$ and acquires a finite width Γ. For energies below the open channel threshold, i.e., $E < 0$, $\mathcal{A}(E)$ is purely real and $\Gamma(E) = 0$. In the low-energy limit, $k \to 0$, Eq. (26) reduces to

$$\mathcal{A}(E) = \Delta - iCk, \tag{27}$$

where C is a constant characterizing the coupling strength between $\mathcal{P}$ and $\mathcal{Q}$ space [10], given by $C = A(2\kappa_P|\epsilon_P|)^{-1}$ and $\Delta = A(2|\epsilon_P|)^{-1}$. Note that if the direct interaction is resonant, $|a_{\rm bg}| \gg r_0$, the energy dependence of the complex energy shift is given by [28] $\mathcal{A}(E) = \Delta - iCk(1+ika^P)^{-1}$, where $a^P = \kappa_P^{-1}$, yielding an energy dependence of the resonance shift.

Since we consider one open channel, the (elastic) S-matrix element can be written as $e^{2i\delta(k)}$, where $\delta(k)$ is the scattering phase shift. The scattering length, defined as the limit $a \equiv -\tan\delta(k)/k$ ($k \to 0$), is found to be Eq. (3) which shows the well-known dispersive behavior. The direct scattering process is described by the scattering length $a_{\rm bg} = a_{\rm bg}^P + a^P$. At magnetic field value B_0, where the *dressed* bound state crosses the threshold of the entrance channel, the scattering length has a singularity.

The dressed state can be considered as a (quasi)bound state of the total scattering system. The energy of these states is obtained by finding the poles of the total S matrix Eq. (22). This results in solving

$$(k-i\kappa_P)[E-\epsilon_Q-\mathcal{A}(E)] = 0 \tag{28}$$

for k. Due to the underlying assumptions, this equation is valid only for energies around threshold where the open and closed channel poles dominate. Near threshold, the shifted energy of the uncoupled molecular state, $\epsilon_Q + \Delta$, can be approximated by $\mu_{\rm rel}(B - B_0)$. This allows us to solve Eq. (28) for E, and

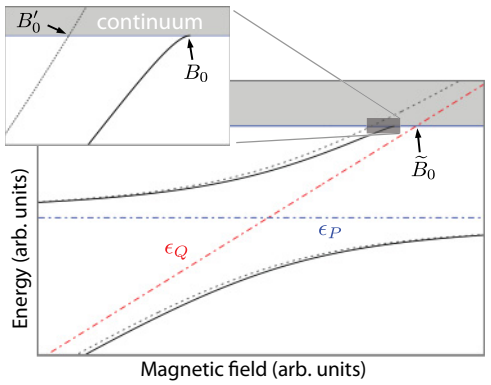

FIG. 6. (Color online) Illustration of the threshold behavior in a (fictitious) two-channel version of the dressed ABM. The threshold behavior is determined by the coupling between the least bound level in the open channel in $\mathcal{P}$ space and the resonant bound level in $\mathcal{Q}$ space. The uncoupled levels are shown as the blue (ϵ_P) and red (ϵ_Q) dash-dotted lines, with ϵ_Q crossing the threshold at $\widetilde{B}_0$. The solid black lines represent the dressed levels, with the upper branch crossing the threshold at B_0. Near the threshold, the dressed level shows the characteristic quadratic dependence on $(B - B_0)$ (see inset). For pure ABM levels (dotted gray) no threshold effects occur and the coupled bound state crosses the threshold at B_0'.

we readily obtain

$$E = -\left(\frac{2|\epsilon_P|^{3/2}\mu_{\rm rel}(B - B_0)}{A}\right)^2, \tag{29}$$

retrieving the characteristic quadratic threshold behavior of the dressed level as a function of $(B - B_0)$. The energy dependence of the molecular state close to resonance is also given by $E = -\hbar^2/(2\mu a^2)$. This allows us to express the field width of the resonance as $\Delta B = C(a_{\rm bg}\mu_{\rm rel})^{-1}$.

We apply the above Feshbach theory to a (fictitious) two-channel version of the ABM, and the results are shown in Fig. 6. This two-channel system is represented by a symmetric 2×2 Hamiltonian matrix, where there is only one open and one closed channel. The open and closed channel binding energies ϵ_P (ϵ_Q) are given by the diagonal matrix elements, while the coupling is represented by the (identical) off-diagonal matrix elements. The closed channel bound state is made linearly dependent on the magnetic field, while the coupling is taken constant. In addition to ϵ_P and ϵ_Q, we plot the corresponding ABM solution, which in this case is equivalent to a typical two-level avoided crossing solution. The figure now nicely illustrates the evolution from the ABM to the dressed ABM approach, where the latter solutions are found from the two physical solutions of Eq. (28), which are also plotted. Since the dressed ABM solutions account for threshold effects, they show the characteristic quadratic bending toward threshold as a function of magnetic field. From this curvature the resonance width can be deduced.

C. The dressed asymptotic-bound-state model

To illustrate the presented model for a realistic case, we will discuss the ^{6}Li-^{40}K system prepared in the $|f_{\rm Li}m_{f_{\rm Li}}, f_{\rm K}m_{f_{\rm K}}\rangle = |1/2, +1/2, 9/2, -7/2\rangle$ two-body hyperfine state as an example throughout this section. This particular mixture is the energetically lowest spin combination of the $M_F = -3$ manifold, allowing us to consider only one open channel. We note that the model can be utilized in cases containing more open channels.

In order to calculate the width of a Feshbach resonance using the method presented in Sec. IV B, three quantities are required: the binding energy of the open channel, ϵ_P, of the closed channel responsible for the Feshbach resonance, ϵ_Q, and the coupling matrix element $\mathcal{K}$ between the two channels. In the following we will describe how to obtain these quantities from the ABM by two simple basis transformations.

For ultracold collisions the hyperfine and Zeeman interactions determine the threshold of the various channels and thus the partitioning of the Hilbert space into subspaces $\mathcal{P}$ and $\mathcal{Q}$, and therefore a natural basis for our tailored Feshbach formalism consists of the eigenstates of $\mathcal{H}^{\rm int}$. Experimentally a system is prepared in an eigenstate $|\alpha\beta\rangle$ of the internal Hamiltonian $\mathcal{H}^{\rm int}$, which we refer to as the entrance channel (cf. Sec. II A). Performing a basis transformation from the $|\sigma\rangle$ basis to the pair basis $|\alpha\beta\rangle$ allows us to identify the open and closed channel subspaces. The open channel has the same spin structure as the entrance channel.

We now perform a second basis transformation which diagonalizes within $\mathcal{Q}$ space without affecting $\mathcal{P}$ space. We obtain the eigenstates of $\mathcal{H}_{QQ}$ and are able to identify the bound state responsible for a particular Feshbach resonance. The bare bound states of $\mathcal{Q}$ space are defined as $\{|\phi_{Q_1}\rangle, |\phi_{Q_2}\rangle, \ldots\}$ with binding energies $\{\epsilon_{Q_1}, \epsilon_{Q_2}, \ldots\}$. For the one-dimensional $\mathcal{P}$ space, which is unaltered by this transformation, the bare bound state $|\Omega_P\rangle$ of $\mathcal{H}_{PP}$ is readily identified with the binding energy ϵ_P. In the basis of eigenstates of $\mathcal{H}_{PP}$ and $\mathcal{H}_{QQ}$, we easily find the coupling matrix elements between the ith $\mathcal{Q}$ space bound state and the open channel bound state $\langle\phi_{Q_i}|\mathcal{H}_{QP}|\Omega_P\rangle$. This gives the coupling constant $A_i = \langle\phi_{Q_i}|\mathcal{H}_{QP}|\Omega_P\rangle\langle\Omega_P^D|\mathcal{H}_{PQ}|\phi_{Q_i}\rangle = \mathcal{K}^2$ that determines the resonance field B_0 by solving Eq. (28) at threshold,

$$\epsilon_{Q_i}\epsilon_P = \frac{\mathcal{K}^2}{2}. \tag{30}$$

The field width of this Feshbach resonance is proportional to the magnetic field difference between the crossings of the dressed (B_0) and uncoupled $\mathcal{Q}$ bound states ($\widetilde{B}_0$) with threshold since

$$\Delta B = \frac{a^P}{a_{\rm bg}}(B_0 - \widetilde{B}_0) = \frac{1}{a_{\rm bg}}\frac{\mathcal{K}^2}{2\kappa_P|\epsilon_P|\mu_{rel}}. \tag{31}$$

We illustrate the dressed ABM for ^{6}Li-^{40}K in Figs. 7 and 8, for $M_F = -3$. To demonstrate the effect of $\mathcal{H}_{PQ}$, we plotted for comparison both the uncoupled and dressed bound states.[3] Details of near-threshold behavior (gray shaded area in Fig. 7) are shown in Fig. 8 together with the obtained scattering length. We solved the pole equation of the total S matrix Eq. (28) for each Q state and plotted only the physical solutions that cause Feshbach resonances. The dressed bound states show the characteristic quadratic bending near the threshold. We have used C_6 to determine r_0 ($\approx a_{\rm bg}^P$) from Eq. (16).

[3]For clarity only one of the two physical solutions is shown.

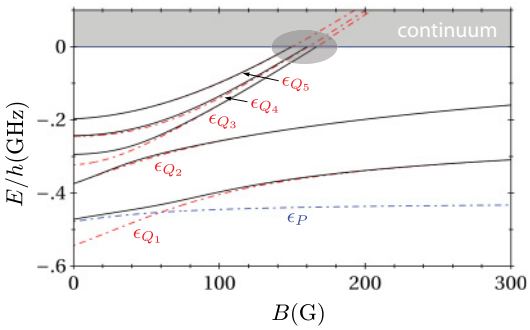

FIG. 7. (Color online) Dressed bound states for ^{6}Li-^{40}K for $M_F = -3$ (black lines; see also Table I). The uncoupled $\mathcal{Q}$ and $\mathcal{P}$ bound states ($\mathcal{H}_{PQ} = \mathcal{H}_{QP} = 0$) are represented by the dot-dashed lines (red and blue, respectively). The gray shaded area is shown in detail in Fig. 8.

Table I summarizes the results of the dressed ABM for the ^{6}Li-^{40}K mixture. Note that the position of the Feshbach resonances will be slightly different compared to the results from the regular ABM, for equal values of $\epsilon_v^{S,0}$. Therefore, we have again performed a χ^2 analysis and we found new values of the binding energies $\epsilon^0/h = 713$ MHz and $\epsilon^1/h = 425$ MHz, which yield a lower χ^2 minimum as compared to the regular ABM calculation.

The obtained value of ΔB generally underestimates the field width of a resonance. This originates from the fact that only the dominant bound state pole corresponding to a^P has been taken into account. By including the pole of the dominant *virtual* state in the Mittag-Leffler expansion, the coupling between the open and closed channels will increase, and hence, ΔB will increase.

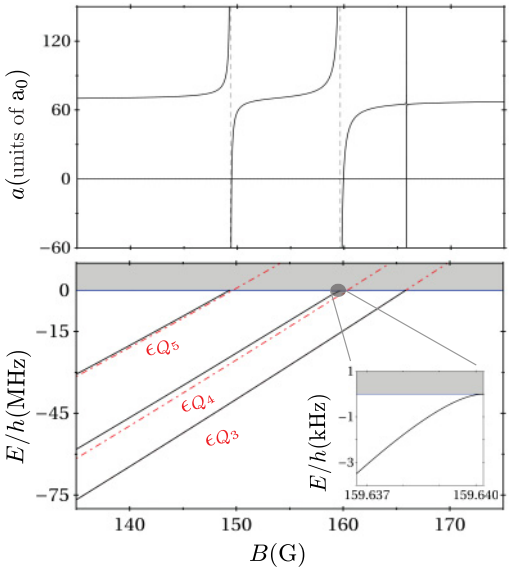

FIG. 8. (Color online) A zoom of the dressed ABM as shown in Fig. 7. The dressed molecular states are shown near threshold (black). The field width of a resonance is related to the magnetic field difference between where the dressed and uncoupled $\mathcal{Q}$ bound states cross the threshold.

TABLE I. The positions of all experimentally observed s-wave Feshbach resonances of ^{6}Li-^{40}K. Column 2 gives the ^{6}Li ($m_{f_{\rm Li}}$) and ^{40}K ($m_{f_{\rm K}}$) hyperfine states. For all resonances $f_{\rm Li} = 1/2$ and $f_{\rm K} = 9/2$. Note that the experimental width of the loss feature $\Delta B_{\rm expt}$ is not the same as the field width ΔB of the scattering length singularity. Feshbach resonance positions B_0 and widths ΔB for ^{6}Li-^{40}K as obtained by the dressed ABM, obtained by minimizing χ^2. The last two columns show the results of full coupled-channel (CC) calculations. All magnetic fields are given in gauss. The experimental and CC values for $M_F < 0$ and $M_F > 0$ are taken from Refs. [8] and [9], respectively. The resonances marked with * have also been studied in Refs. [29,30].

		Experiment		ABM+		CC	
M_F	$m_{f_{\rm Li}}$,$m_{f_{\rm K}}$	B_0	$\Delta B_{\rm expt}$	B_0	ΔB	B_0	ΔB
−5	$-\frac{1}{2}, -\frac{9}{2}$	215.6	1.7	216.2	0.16	215.6	0.25
−4	$+\frac{1}{2}, -\frac{9}{2}$	157.6	1.7	157.6	0.08	158.2	0.15
−4	$+\frac{1}{2}, -\frac{9}{2}$	168.2*	1.2	168.5	0.08	168.2	0.10
−3	$+\frac{1}{2}, -\frac{7}{2}$	149.2	1.2	149.1	0.12	150.2	0.28
−3	$+\frac{1}{2}, -\frac{7}{2}$	159.5	1.7	159.7	0.31	159.6	0.45
−3	$+\frac{1}{2}, -\frac{7}{2}$	165.9	0.6	165.9	0.0002	165.9	0.001
−2	$+\frac{1}{2}, -\frac{5}{2}$	141.7	1.4	141.4	0.12	143.0	0.36
−2	$+\frac{1}{2}, -\frac{5}{2}$	154.9*	2.0	154.8	0.50	155.1	0.81
−2	$+\frac{1}{2}, -\frac{5}{2}$	162.7	1.7	162.6	0.07	162.9	0.60
+5	$+\frac{1}{2}, +\frac{9}{2}$	114.47(5)	1.5(5)	115.9	0.91	114.78	1.82

V. SUMMARY AND CONCLUSION

We have presented a model to accurately describe Feshbach resonances. The model allows for fast and accurate prediction of resonance positions and widths with very little experimental input. The reduction of the basis to only a few states allows us to describe Feshbach resonances in a large variety of systems without accurate knowledge of scattering potentials.

Using the ABM in combination with the accumulated phase method allows a description of Feshbach resonances in alkali-metal systems with a large degree of accuracy, using only three input parameters. Additionally, the fast computational time of the model allows us to map all available Feshbach resonances in a system and select the optimal resonance required to perform a certain experiment. For the ^{6}Li-^{40}K mixture we have utilized this ability to find a broad resonance as presented in Ref. [9]. In addition, locating, e.g., overlapping resonances in multicomponent (spin) mixtures can be performed easily using the ABM.

An additional important feature is that the model can be stepwise extended to include more phenomena allowing more complex systems described. For example, a possible extension would be to include the contribution of the dominant virtual state in the Mittag-Leffler expansion; this would allow for an accurate description of the resonance widths for systems with a large and negative $a_{\rm bg}$. Additionally, inclusion of the dipole-dipole interaction allows a description of systems where Feshbach resonances occur due to dipole-dipole coupling. Finally, it has already been shown by Tscherbul *et al.* [31] that the ABM can be successfully extended by including

coupling to bound states by means of an externally applied radio-frequency field.

The approach as described in the ABM is in principle not limited to two-body systems. Magnetic-field-induced resonances in, e.g., dimer-dimer scattering have already been experimentally observed [32]. For few-body systems an approach without having to solve the coupled radial Schrödinger equations is very favorable. This large variety of unexplored features illustrate the richness of the model.

ACKNOWLEDGMENTS

This work is part of the research program on Quantum Gases of the Stichting voor Fundamenteel Onderzoek der Materie (FOM), which is financially supported by the Nederlandse Organisatie voor Wetenschappelijk Onderzoek (NWO).

[1] For reviews see *Proceedings of the International School of Physics "Enrico Fermi," Course CLXIV, Varenna, 20–30 June 2006*, edited by M. Inguscio, W. Ketterle, and C. Salomon (IOS Press, Amsterdam, 2008).
[2] I. Bloch, J. Dalibard, and W. Zwerger, Rev. Mod. Phys. **80**, 885 (2008).
[3] C. Chin, R. Grimm, P. Julienne, and E. Tiesinga, Rev. Mod. Phys. **82**, 1225 (2010).
[4] H. T. C. Stoof, J. M. V. A. Koelman, and B. J. Verhaar, Phys. Rev. B **38**, 4688 (1988).
[5] M. Houbiers, H. T. C. Stoof, W. I. McAlexander, and R. G. Hulet, Phys. Rev. A **57**, R1497 (1998).
[6] J. M. Vogels, B. J. Verhaar, and R. H. Blok, Phys. Rev. A **57**, 4049 (1998).
[7] T. M. Hanna, E. Tiesinga, and P. S. Julienne, Phys. Rev. A **79**, 040701 (2009).
[8] E. Wille *et al.*, Phys. Rev. Lett. **100**, 053201 (2008).
[9] T. G. Tiecke, M. R. Goosen, A. Ludewig, S. D. Gensemer, S. Kraft, S. J. J. M. F. Kokkelmans, and J. T. M. Walraven, Phys. Rev. Lett. **104**, 053202 (2010).
[10] A. J. Moerdijk, B. J. Verhaar, and A. Axelsson, Phys. Rev. A **51**, 4852 (1995).
[11] C. A. Stan, M. W. Zwierlein, C. H. Schunck, S. M. F. Raupach, and W. Ketterle, Phys. Rev. Lett. **93**, 143001 (2004).
[12] P. Julienne (private communication).
[13] M. R. Goosen, T. G. Tiecke, W. Vassen, and S. J. J. M. F. Kokkelmans, Phys. Rev. A **82**, 042713 (2010).
[14] E. Tiesinga, A. J. Moerdijk, B. J. Verhaar, and H. T. C. Stoof, Phys. Rev. A **46**, R1167 (1992).
[15] B. J. Verhaar, E. G. M. van Kempen, and S. J. J. M. F. Kokkelmans, Phys. Rev. A **79**, 032711 (2009).
[16] R. J. LeRoy and R. B. Bernstein, J. Chem. Phys. **52**, 3869 (1970).
[17] A. S. Jensen, K. Riisager, D. V. Fedorov, and E. Garrido, Rev. Mod. Phys. **76**, 215 (2004).
[18] B. Gao, Phys. Rev. A **58**, 1728 (1998), describes analytical solutions.
[19] B. M. Smirnov and M. I. Chibisov, Zh. Eksp. Teor. Fiz. **48**, 939 (1965) [Sov. Phys. JETP **21**, 624 (1965)].
[20] H. Salami, A. J. Ross, P. Crozet, W. Jastrzebski, P. Kowalczyk, and R. J. L. Roy, J. Chem. Phys. **126**, 194313 (2007).
[21] M. Aymar and O. Dulieu, J. Chem. Phys. **122**, 204302 (2005).
[22] A. Derevianko, J. F. Babb, and A. Dalgarno, Phys. Rev. A **63**, 052704 (2001).
[23] A. Pashov, O. Docenko, M. Tamanis, R. Ferber, H. Knöckel, and E. Tiemann, Phys. Rev. A **76**, 022511 (2007).
[24] J. P. S., Faraday Discuss. **142**, 361 (2009).
[25] H. Feshbach, Ann. Phys. **5**, 357 (1958).
[26] H. Feshbach, Ann. Phys. **19**, 287 (1962).
[27] B. Marcelis, E. G. M. van Kempen, B. J. Verhaar, and S. J. J. M. F. Kokkelmans, Phys. Rev. A **70**, 012701 (2004).
[28] B. Marcelis and S. J. J. M. F. Kokkelmans, Phys. Rev. A **74**, 023606 (2006).
[29] A.-C. Voigt, M. Taglieber, L. Costa, T. Aoki, W. Wieser, T. W. Hänsch, and K. Dieckmann, Phys. Rev. Lett. **102**, 020405 (2009).
[30] F. M. Spiegelhalder, A. Trenkwalder, D. Naik, G. Kerner, E. Wille, G. Hendl, F. Schreck, and R. Grimm, Phys. Rev. A **81**, 043637 (2010).
[31] T. V. Tscherbul, T. Calarco, I. Lesanovsky, R. V. Krems, A. Dalgarno, and J. Schmiedmayer, Phys. Rev. A **81**, 050701 (2010).
[32] C. Chin, T. Kraemer, M. Mark, J. Herbig, P. Waldburger, H.-C. Nägerl, and R. Grimm, Phys. Rev. Lett. **94**, 123201 (2005).